

Probing the catalytic site of rabbit muscle glycogen phosphorylase using a series of specifically modified maltohexaose derivatives

Makoto Nakamura¹ · Yasushi Makino¹  · Chika Takagi¹ · Tohru Yamagaki² · Masaaki Sato¹

Received: 23 March 2017 / Revised: 12 May 2017 / Accepted: 15 May 2017 / Published online: 8 June 2017
© Springer Science+Business Media New York 2017

Abstract Glycogen phosphorylase (GP) is an allosteric enzyme whose catalytic site comprises six subsites (SG₁, SG₋₁, SG₋₂, SG₋₃, SG₋₄, and SP) that are complementary to tandem five glucose residues and one inorganic phosphate molecule, respectively. In the catalysis of GP, the nonreducing-end glucose (Glc) of the maltooligosaccharide substrate binds to SG₁ and is then phosphorylated to yield glucose 1-phosphate. In this study, we probed the catalytic site of rabbit muscle GP using pyridylaminated-maltohexaose (Glcα1–4Glcα1–4Glcα1–4Glcα1–4GlcPA, where GlcPA = 1-deoxy-1-[(2-pyridyl)amino]-D-glucitol]; abbreviated as PA-0) and a series of specifically modified PA-0 derivatives (Glc_m-AltNAc-Glc_n-GlcPA, where $m + n = 4$ and AltNAc is 3-acetoamido-3-deoxy-D-altrose). PA-0 served as an efficient substrate for GP, whereas the other PA-0 derivatives were not as good as the PA-0, indicating that substrate recognition by all the SG₁–SG₋₄ subsites was important for the catalysis of GP. By comparing the initial reaction rate toward the PA-0 derivatives ($V_{\text{derivative}}$) with that toward PA-0 ($V_{\text{PA-0}}$), we found that the value of $V_{\text{derivative}}/V_{\text{PA-0}}$ decreased significantly as the level of allosteric activation of GP increased. These results suggest that some conformational changes have taken place in the maltooligosaccharide-binding region of the GP catalytic site during allosteric regulation.

Keywords Glycogen · Glycogen phosphorylase · Modified maltooligosaccharide · Pyridylamination · Substrate recognition

Abbreviations

AltNAc	3-acetoamido-3-deoxy-D-altrose
CD	Cyclodextrin
CP-91149	[<i>R</i> -(<i>R</i> *, <i>S</i> *)]-5-chloro- <i>N</i> -[3-(dimethylamino)-2-hydroxy-3-oxo-1-(phenylmethyl)propyl]-1 <i>H</i> -indole-2-carboxamide
DHB	2,5-dihydroxybenzoic acid
GDE	Glycogen debranching enzyme
Glc	D-glucose
Glc-1-P	α-D-glucose 1-phosphate
GlcPA	1-deoxy-1-[(2-pyridyl)amino]-D-glucitol
GP	Glycogen phosphorylase
HPLC	High-performance liquid chromatography
MALDI-TOF MS	Matrix-assisted laser desorption/ionization time-of-flight mass spectrometry
MW	Molecular weight
α-NH ₂ -CD	3A-amino-3A-deoxy-(2AS,3AS)-α-cyclodextrin
PA	Pyridylamino
P _i	Inorganic phosphate

✉ Yasushi Makino
ymakino@c.s.osakafu-u.ac.jp

¹ Department of Chemistry, Graduate School of Science, Osaka Prefecture University, Gakuen-cho 1-1, Naka-ku, Sakai, Osaka 599-8531, Japan

² Bioorganic Research Institute, Suntory Foundation for Life Sciences, Seika-cho, Soraku-gun, Kyoto 619-0284, Japan

Introduction

Glycogen (MW, 10⁶–10⁷) is a highly-branched polymer of D-glucose (Glc) synthesized on a glycogenin primer [1–3]. In the

glycogen molecule, most of the Glc residues are polymerized through α 1-4-glycosidic linkages; however, approximately 5%–10% of Glc residues also make an α 1-6-glycosidic bond, resulting in α 1-6-branching. When an animal body requires energy, glycogen is rapidly broken down by the combined activity of glycogen phosphorylase (GP) (EC, 2.4.1.1; MW, 1.9×10^5) and glycogen debranching enzyme (GDE) (EC, 2.4.1.25 and 3.2.1.33; MW, 1.6×10^5) [4–8]. GP is reported to remove α 1-4-Glc residues from the outermost chains of the glycogen molecule until 4 Glc residues remain on either side of the α 1-6-branching [9, 10]. This reaction, called phosphorylase, proceeds by the consumption of inorganic phosphate (P_i) and results in the formation of glucose 1-phosphate (Glc-1-P) and GP-limit dextrin. GP is present in two interconvertible forms, GP_a (phosphorylated form, middle activity) and GP_b (nonphosphorylated form, low activity) [9–11]. Muscle GP activity is regulated by the interconversion of GP_a and GP_b and by the binding of a number of allosteric effectors, including AMP, ATP, and glucose 6-phosphate (Glc-6-P) [12]. The most highly activated forms of muscle GP are AMP-bound, regardless of the phosphorylation state [11, 13, 14]. Although the binding sites for these effectors have been well characterized by kinetic and X-ray crystallographic methods [12], sufficient structural and functional information on the catalytic site is not available. This is because GP does not or hardly exhibits reactivity with maltotetraose (Glc₄-OH) or smaller maltooligosaccharides [15], and oligosaccharides have never been observed to bind at the GP catalytic site in X-ray crystallographic analyses [16–18].

The catalytic sites of dextrin-degrading enzymes have been probed using a series of maltooligosaccharides (Glc_{*n*}-OH) or methyl α -maltooligosides (Glc_{*n*}-OCH₃) with various chain lengths [19–22]. Unlike GP, most of the dextrin-degrading enzymes exhibit a significant activity even toward maltotetraose (Glc₄-OH) or smaller maltooligosaccharides (*e.g.*, α -glucosidase and glucoamylase). For endo-enzymes (*e.g.*, α -amylase), cyclodextrins having one modified sugar residue (*e.g.*, 6-*O*-tosyl-Glc, 2,3-anhydro-(3*R*)-Glc, or 6-deoxy-6-iodo-Glc) were also used as the probes [23, 24], and from the reaction product, the oligosaccharide substrate specificity of the catalytic site has been elucidated. A series of specifically modified linear maltooligosaccharides (Glc_{*m*}-X-Glc_{*n*}-OH, where $m + n$ is constant and X is a modified sugar residue) were thought to be effective substrates to characterize the catalytic sites of long-chain-specific exo-enzymes (*e.g.*, GP); however, preparation of a series of Glc_{*m*}-X-Glc_{*n*}-OH compounds was difficult.

To obtain new information on the structure and function of the GP catalytic site, we first prepared a series of specifically modified linear maltooligosaccharides and then analyzed the kinetics of the GP activity on these synthetic substrates. Based on the structure of GP-limit dextrin, it is widely accepted that the GP catalytic site accommodates a maltopentaosyl- (Glc α 1-4Glc α 1-4Glc α 1-4Glc α 1-4Glc α 1-)

residue comprising the nonreducing-end [9, 10, 15, 25]. In this study, we used pyridylaminated (PA-) maltohexaose (Glc α 1-4Glc α 1-4Glc α 1-4Glc α 1-4Glc α 1-4GlcPA, where GlcPA = 1-deoxy-1-[(2-pyridyl)amino]-D-glucitol; abbreviated as PA-0) as a standard maltooligosaccharide substrate [26–28]. Pyridylation of the reducing-end provided us excellent separation and very sensitive detection of oligosaccharides [29, 30]; therefore, we were able to prepare a series of specifically modified PA-0 derivatives (Glc_{*m*}-AltNAc-Glc_{*n*}-GlcPA, where $m + n = 4$, AltNAc = 3-acetoamido-3-deoxy-D-altriose) using 3A-amino-3A-deoxy-(2*AS*,3*AS*)- α -cyclodextrin (α -NH₂-CD) as the starting material. Although the AltNAc residue is slightly larger than the Glc residue and has different side-chain orientations at the C2 and C3 positions, there may be a unique interaction between the AltNAc residue and the GP catalytic site. The substrates having four Glc residues and one AltNAc residue within the pentasaccharide moiety on the nonreducing-end side made it possible to evaluate the importance of each subsite in the maltooligosaccharide-binding region of the GP catalytic site [31, 32].

Materials and methods

Materials

Maltohexaose, 2-aminopyridine, and Wakosil-II 5C18 HG columns (4.6 \times 150 mm and 10.0 \times 250 mm) were purchased from Wako Pure Chemicals (Osaka, Japan). α -NH₂-CD was purchased from Tokyo Chemical Industry (Tokyo, Japan). Rabbit muscle glycogen phosphorylase a (GP_a), glycogen phosphorylase b (GP_b), AMP, 2,5-dihydroxybenzoic acid (DHB), and [*R*-(*R**,*S**)]-5-chloro-*N*-[3-(dimethylamino)-2-hydroxy-3-oxo-1-(phenylmethyl)propyl]-1*H*-indole-2-carboxamide (CP-91149) were purchased from Sigma-Aldrich (St. Louis, MO, USA). Shodex NH2P-50 columns (4.6 \times 150 mm and 4.6 \times 250 mm) came from Showa Denko (Tokyo, Japan) and Silica gel 60 aluminum sheets from Merck (Darmstadt, Germany). Dowex 50W-X2 (100–200 mesh) came from Dow Chemical Company (Midland, MI, USA), and Toyopearl HW-40F from Tosoh (Tokyo, Japan).

GP_a and GP_b were purified according to previously described methods [33]. PA-maltooligosaccharides (Glc_{*n*}-GlcPA; $n = 0$ –6) and methyl α -maltooligosides (Glc_{*n*}-OCH₃; $n = 1$ –6) were prepared as reported previously [28].

High-performance liquid chromatography (HPLC) of PA-oligosaccharides

Standard size-fractionation HPLC of PA-oligosaccharides was performed on a Shodex NH2P-50 column (4.6 \times 150 mm) at a flow rate of 0.9 mL/min at 25 °C [30]. The eluent was acetonitrile:water:acetic acid (750:250:3, v/v/v), which was

titrated to pH 7.0 with 5.0% aqueous ammonia. PA-oligosaccharides were detected by fluorescence (excitation wavelength, 320 nm; emission wavelength, 400 nm).

High-resolution size-fractionation HPLC of PA-oligosaccharides was performed on a Shodex NH2P-50 column (4.6 × 250 mm) [30]. Conditions were the same as those for standard size-fractionation HPLC except the eluent was acetonitrile:water:acetic acid (730:270:3, v/v/v) titrated to pH 7.0 with 5.0% aqueous ammonia.

Reversed-phase HPLC of PA-oligosaccharides was performed using a Wakosil-II 5C18 HG column (10.0 × 250 mm) and elution with 50 mM ammonium acetate buffer (pH 4.8) at 25 °C at a flow rate of 3.0 mL/min [34]. PA-oligosaccharides were detected by fluorescence (excitation wavelength, 320 nm; emission wavelength, 400 nm).

Preparation of PA-0 derivatives

α -NH₂-CD (300 mg) was dissolved in 10 mL of saturated sodium bicarbonate solution and then 500 μ L of acetic anhydride was added to the solution [30]. After 5 min, another 10 mL of sodium bicarbonate solution and 500 μ L of acetic anhydride were added, and the solution was left at room temperature for 30 min. Dowex 50W–X2 resin (H⁺ form) was then added to the solution to bring the pH to about 3. The mixture was filtered, and the resin was washed with five column volumes of water. The whole eluate collected was lyophilized, and the *N*-acetylated product (α -NHAc-CD) was obtained with a yield of 92%.

Next, α -NHAc-CD was dissolved in 30 mL of 0.1 M hydrochloric acid, and the mixture was heated at 90 °C for 13 min. Acid hydrolysis was stopped at an early stage to suppress the formation of lower molecular weight dextrans. To remove *N*-deacetylated dextrans completely, the partial acid hydrolysate was applied to a Dowex 50W–X2 column (25 × 200 mm, H⁺ form) [30]. The resin was washed with five column volumes of water, and the whole eluate collected was neutralized with 1 M NaOH. The solution was then concentrated to dryness under reduced pressure. The residue was dissolved in a small volume of water and desalted by gel-filtration on the Toyopearl HW 40F column (25 × 350 mm) equilibrated with 10 mM ammonium acetate buffer, pH 6.0. Elution was monitored by TLC using Silica gel 60 aluminum sheets. The TLC eluent was 2-butanone:acetic acid:water, 3:1:1 (v/v/v), and the developing reagent was 5% sulfuric acid in methanol. The dextrin fractions were combined and lyophilized.

Pyridylamination of the dextrans was performed as follows [27]. The lyophilized sample was dissolved in a mixture of 1.5 mL of acetic acid and 4.2 g of 2-aminopyridine, and the resulting solution was heated at 90 °C for 60 min. Next, 18.3 mL of a reducing reagent (prepared by dissolving 20 g of borane-dimethylamine complex in 8.0 mL acetic acid and 5.0 mL water) was added, and the reaction mixture was heated

at 80 °C for 35 min. Five milliliters of 1.0% aqueous ammonia was added to the reaction mixture, and excess reagents were removed by extraction three times with 20 mL of chloroform. The water layer was then concentrated to dryness under a reduced pressure. The residue was dissolved in a small volume of water and then separated by gel-filtration on a Toyopearl HW 40F column (3.5 × 140 cm) equilibrated with 10 mM ammonium acetate buffer (pH 6.0). The eluate was collected in 10-mL fractions, and each fraction was analyzed by standard size-fractionation HPLC. Fractions containing PA-hexasaccharides were collected and lyophilized.

Separation of PA-hexasaccharides was performed as follows. To remove shorter PA-oligosaccharides completely, the lyophilized sample was dissolved in a small amount of water and separated using standard size-fractionation HPLC, and the PA-hexasaccharide fraction was collected (Fig. 1-i). This fraction was then further fractionated into Fractions A–E using reversed-phase HPLC (Fig. 1-ii). Fraction B was fractionated into Fractions B1 and B2 using high-resolution size-fractionation HPLC (Fig. 1-iii). In addition, each fraction was further purified 2 times by the combination of reversed-phase and high-resolution size-fractionation HPLCs. The yields of PA-hexasaccharides PA-1 (Fraction E), PA-2 (Fraction B2), PA-3 (Fraction C), PA-4 (Fraction D), PA-5 (Fraction B1), and PA-6 (Fraction A) were 0.04, 0.09, 0.4, 0.4, 0.8, and 0.2 μ mol, respectively (Table 1). Each substrate purified showed a single peak by HPLC enough for measuring enzyme activity.

Matrix-assisted laser desorption/ionization time-of-flight mass spectrometry (MALDI-TOF MS) and tandem MS/MS analyses

All MALDI-TOF MS and MS/MS spectra were acquired with an Ultraflex III MALDI-TOF/TOF MS instrument (Bruker Daltonics, Co., GmbH, Germany) under the same experimental conditions. A matrix of 2,5-dihydroxybenzoic acid (DHB) was dissolved in 80% acetonitrile aqueous solution at a final concentration of 10 mg/mL. A sample aliquot and 1 μ L DHB were deposited on the target and allowed to dry. The predominant molecular-related ions were obtained as sodium adduct molecules $[M + Na]^+$ to estimate their exact masses. The tandem MS/MS spectra were measured from the protonated molecule $[M + H]^+$ because the PA-sugars had the protonated charge at the reducing-end, and the sequential fragment ions were obtained to elucidate the structures of the chemically prepared PA-sugars.

Sensitive GP assay in the direction of glycogen degradation

A mixture (70 μ L) containing 40 mM sodium phosphate buffer (pH 6.8), 35 μ M PA-hexasaccharide, 1.0 mM β -mercaptoethanol, 0 or 1.0 mM AMP, 0.05% gelatin, and 5–

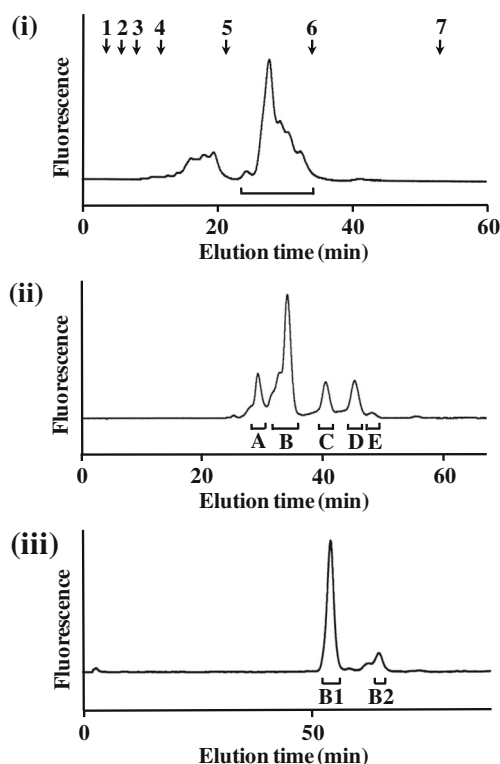


Fig. 1 Isolation of PA-0 derivatives by preparative HPLC. α -NHAc-CD was partially hydrolyzed with hydrochloric acid, and the hydrolysate was pyridylaminated. The PA-oligosaccharide mixture obtained was subjected to HPLC as described in *Materials and methods*. (i) Size-fractionation HPLC of the PA-oligosaccharide mixture from α -NHAc-CD. The arrows 1–7 indicate the elution positions of standard PA-maltooligosaccharides (GlcPA–Glc₆–GlcPA). PA-hexasaccharide fraction was collected as indicated by the bar. (ii) Reversed-phase HPLC of the PA-hexasaccharide fraction. Fractions A–E were collected as indicated by the bars. (iii) High-resolution size-fractionation HPLC of Fraction B. Fractions B1 and B2 were collected as indicated by the bars. Each fraction was further purified two times by the combination of reversed-phase and high-resolution size-fractionation HPLCs

500 nM rabbit muscle GP (*i.e.*, 0.01–1 μ M GP subunit) was incubated at 37 °C for 30 min. To stop the reaction, the mixture was heated at 100 °C for 5 min. After heating, the resulting PA-pentasaccharide was isolated and quantified by standard size-fractionation HPLC. Although the PA-hexasaccharide concentration was very low, it was considered to be constant throughout the enzymatic reaction because the chain-shortened product could be isolated and quantified even at 10 fmol, and at the end of the reaction period, >95% of the PA-hexasaccharide did not react and remained unchanged.

Evaluation of the kinetic parameters of AMP-activated GPb

Apparent K_m and V_{max} values were calculated according to the method of Lineweaver and Burk [35]. Methyl α -maltooligosides

and PA-maltooligosaccharides were used as oligosaccharide substrates. GPb was assayed at constant concentrations of P_i (40 mM) and AMP (1.0 mM) with five different concentrations of oligosaccharide (1, 3, 10, 20, and 30 mM). The chain-shortened products from methyl α -maltooligosides were isolated and quantified by size-fractionation HPLC on a Shodex NH2P-50 column (4.6 \times 150 mm) at a flow rate of 0.9 mL/min. The eluent was a 4:1 (v/v) mixture of acetonitrile and water, and the elution was monitored using a refractive index detector. The chain-shortened products from PA-maltooligosaccharides were isolated and quantified by standard size-fractionation HPLC. The reciprocal initial reaction rates were plotted against reciprocal substrate concentrations, and the data were fitted to the Michaelis–Menten equation by the least-squares method using a computer program.

Estimation of the dissociation constant of GPa–CP-91149 binding

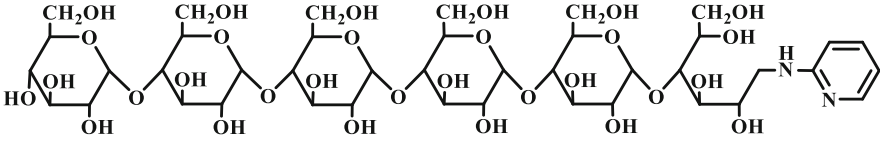
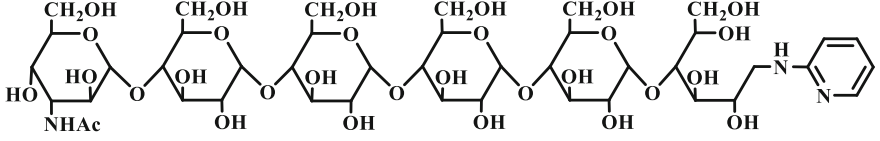
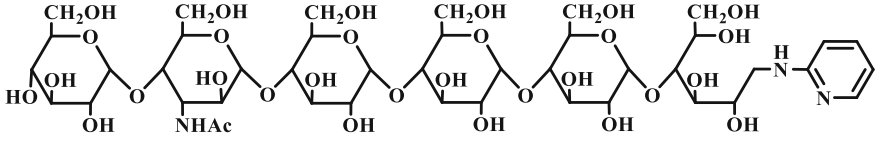
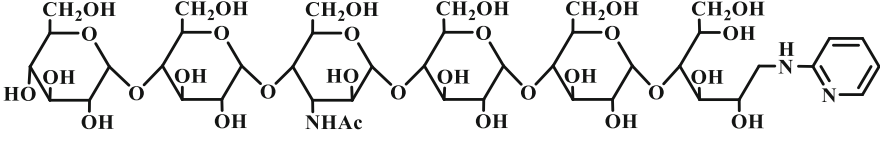
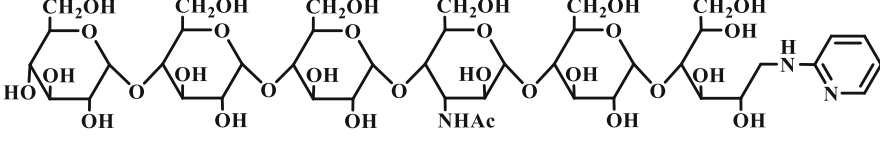
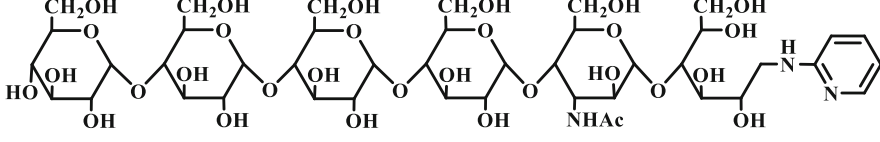
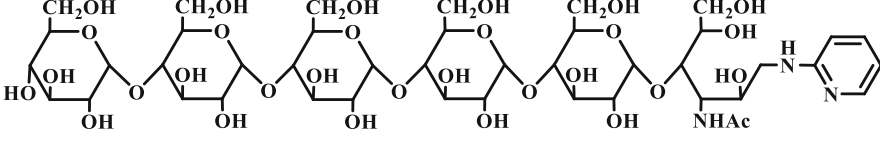
The equilibrium dialysis experiment was performed according to a previously reported method [36]. A mixture (100 μ L) containing 40 mM sodium phosphate buffer (pH 6.8), 2.5 μ M rabbit muscle GPa, 1.0 mM β -mercaptoethanol, 0.05% gelatin, and 10 μ M CP-91149 was prepared, packed in a Fast Micro-Equilibrium DIALYZER (5 \times 10⁴ MWCO membrane), and dialyzed at 10 °C against 100 μ L of buffer solution (40 mM sodium phosphate buffer (pH 6.8), 1.0 mM β -mercaptoethanol, and 0.05% gelatin). After 24 h of dialysis, equilibrium was reached between the internal and external solutions. The CP-91149 concentration in the external solution was analyzed by reversed-phase HPLC using a Wakosil-II 5C18 HG column (4.6 \times 150 mm) at a flow rate of 0.8 mL/min at 25 °C. The column was equilibrated with 50 mM ammonium acetate buffer, pH 4.8, containing 0.1% acetonitrile. After injecting a mixture sample, the concentration of acetonitrile was linearly raised to 40% in 80 min. Elutions were monitored by measuring the absorbance at 280 nm. The apparent dissociation constant, $K_{d,app}$, was calculated as reported previously [36].

Results and discussion

Schematic representation of the GP catalytic site

The most highly activated forms of muscle GP are AMP-bound, regardless of the phosphorylation state [11, 13, 14]. Of these, the AMP-bound GPb is usually used for biochemical research. The catalytic site of AMP-activated GP is composed of six subsites (SG₁, SG₋₁, SG₋₂, SG₋₃, SG₋₄, and SP) that are complementary to tandem five Glc residues (G₁, G₋₁, G₋₂, G₋₃, and G₋₄) and one P_i molecule, respectively [9, 10, 15, 37, 38]. A schematic representation of

Table 1 Structures of PA-maltohexaose (PA-0) and its derivatives

Abbreviation	Structure
PA-0	
PA-1	
PA-2	
PA-3	
PA-4	
PA-5	
PA-6	

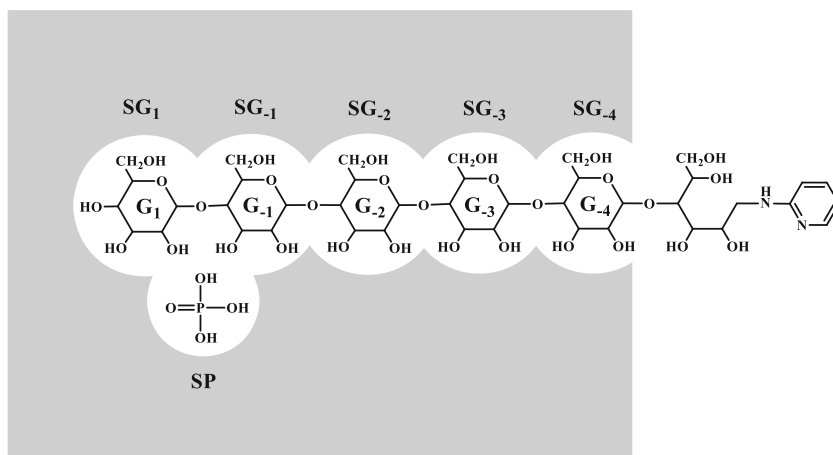
the GP catalytic site is shown in Fig. 2. In the phosphorolysis reaction, the α -1,4-glycosidic linkage between G_1 and G_{-1} is split, forming Glc-1-P. We first analyzed the kinetics of the GP activity toward methyl α -maltopentaoside (Glc₅-OCH₃) and PA-0 in the presence of 1 mM AMP, where the enzyme is well known to be fully activated. The results are summarized in Table 2. Because the apparent K_m and V_{max} values toward PA-0 were similar to those toward methyl

α -maltopentaoside, PA-0 is thought to fit all of the SG₁–SG₋₄ subsites in a suitable state.

Preparation of a series of specifically modified PA-0 derivatives

Many GP researchers have believed that SG₁ (glycone-binding region) plays the most important role in the binding

Fig. 2 Schematic representation of the productive binding of PA-0 and P₁ to the GP catalytic site. The GP catalytic site is composed of six subsites (SG₁, SG₋₁, SG₋₂, SG₋₃, SG₋₄, SP); SG₁ and SP are for nonreducing-end Glc and P₁, respectively. When G₁, G₋₁, G₋₂, G₋₃, and G₋₄ of the maltooligosaccharide substrate and P₁ interact with subsites SG₁, SG₋₁, SG₋₂, SG₋₃, SG₋₄, and SP, respectively, the α-1,4-glycosidic linkage between G₁ and G₋₁ is phosphorylated



of the maltooligosaccharide substrate to the GP catalytic site [5, 17, 18, 37], while roles of the SG₋₁–SG₋₄ subsites (aglycone-binding region) have only received a minimal amount of attention. By comparing the initial reaction rates toward the specifically modified PA-0 derivatives with those toward PA-0, we wish to discuss the importance of each Glc residue (G₁, G₋₁, G₋₂, G₋₃, or G₋₄) of PA-0 for the catalytic action of GP (Fig. 2). A series of specifically modified PA-0 derivatives containing four Glc residues, one AltNAc residue, and one reducing-end GlcPA residue (Glc_m-AltNAc-Glc_n-GlcPA, where $m + n = 4$) were prepared as described in *Materials and methods*. We then obtained all the PA-0 derivatives containing one AltNAc residue as summarized in Table 1. The structures of the prepared PA-0 derivatives were proved from their exact masses by MALDI-TOF MS spectra as sodium adduct molecules $[M + Na]^+$ at m/z 1132.4 (Fig. 3). The positions of the AltNAc residue in the PA-0 derivatives were identified by tandem MS/MS spectra from the protonated molecules $[M + H]^+$ (Fig. 4). The five prepared hexaoses AltNAc-Glc₄-GlcPA (PA-1), Glc-AltNAc-Glc₃-GlcPA (PA-2), Glc₂-AltNAc-Glc₂-GlcPA (PA-3), Glc₃-AltNAc-Glc-GlcPA (PA-4), and Glc₄-AltNAc-GlcPA (PA-5) were used as

oligosaccharide substrates to evaluate the importance of each Glc residue (G₁, G₋₁, G₋₂, G₋₃, or G₋₄) of PA-0 for the catalytic action of GP.

Kinetics of GP activity toward various PA-oligosaccharides

Three levels of allosteric regulation of muscle GP have been identified: GPb (nonphosphorylated form, low activity), GPa (phosphorylated form, middle activity), and AMP-bound GP (high activity) [11, 13, 14]. Of these, nonactivated GPb has been considered difficult to assay because $1/K_m$ and V_{max} values for the nonactivated GPb are much smaller than those for the AMP-activated GP [39]. However, in this study, our fluorescent-labeled oligosaccharide allowed detection of a very small amount of the reaction product. For instance, PA-maltopentaose, the product from PA-maltohexaose, was isolated and quantified at 10 fmol using HPLC equipped with a fluorescent spectrophotometer (data not shown). Thus, we assayed the rabbit muscle GP activity at these three levels of allosteric regulation using various PA-oligosaccharides as substrates. The results are summarized in Table 3. When the initial reaction rate toward PA-0 was taken as unity, the relative initial reaction rates toward Glc₃-GlcPA and Glc₄-GlcPA were much smaller than 1 at any level of allosteric regulation. In addition, the relative initial reaction rates toward PA-1–PA-5 were also very small, particularly toward PA-1. These results indicate that all tandem five Glc residues (G₁, G₋₁, G₋₂, G₋₃, and G₋₄) are important for the catalysis of GP (Fig. 2). It should be noted that the relative initial reaction rates toward PA-5 (Glc₄-AltNAc-GlcPA) and those toward Glc₄-GlcPA were in the similar range at any level of allosteric activation. Although the role of the AltNAc residue is not clear currently, it is certain that the AltNAc residue does not have any positive effect on specific recognition by the GP subsites. The AltNAc residue does not strongly bind to SG₁, SG₋₁, SG₋₂, SG₋₃, or SG₋₄ as the native Glc does. Thus, our results suggest that, as

Table 2 Kinetic parameters of AMP-activated GPb

Maltooligosaccharide substrate	Apparent V_{max} ($\mu\text{mol}/(\text{min}\cdot\text{mg protein})$)	Apparent K_m (mM)
Glc ₄ -OCH ₃	— ^a	— ^a
Glc ₅ -OCH ₃	20 ± 3	12 ± 2
Glc ₆ -OCH ₃	21 ± 3	11 ± 2
Glc ₄ -GlcPA	— ^a	— ^a
Glc ₅ -GlcPA (PA-0)	19 ± 3	13 ± 2
Glc ₆ -GlcPA	21 ± 3	11 ± 2

^a The value was not determined, because the enzyme showed very low activity (less than 1 $\mu\text{mol}/(\text{min}\cdot\text{mg protein})$) at 10 mM maltooligosaccharide substrate)

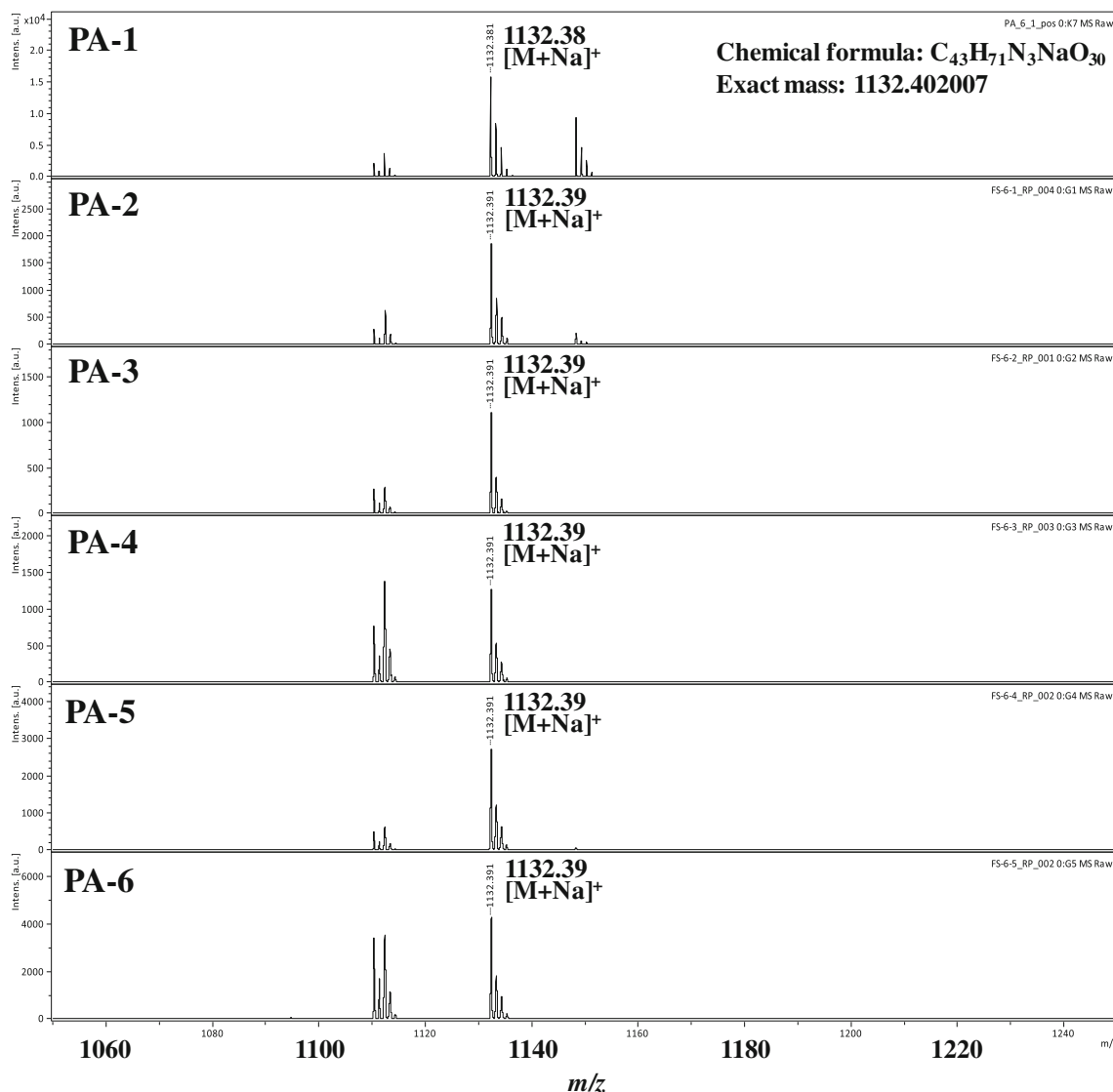


Fig. 3 MALDI-TOF MS spectra of specifically modified PA-0 derivatives. The chemically synthesized derivatives PA-1, PA-2, PA-3, PA-4, PA-5, and PA-6 have one AltNAc residue at different positions of the oligosaccharide

has been believed by many GP researchers [5, 17, 18, 37], the interaction between the G_1 residue and the SG_1 subsite is very important. Although the interaction between the G_{-4} residue and the SG_{-4} subsite seems to be less important than the other interactions, it still has some role in the catalytic action of GP since in the case of Glc_4 -GlcPA, the initial reaction rate of AMP-activated GPb decreased down to approximately 1.5%. Therefore, although the GP catalytic site has relatively high K_m values toward maltooligosaccharide substrates (Table 2), substrate recognition by all the SG_1 – SG_{-4} subsites is important for the catalysis of GP [40]. Because the structure of AltNAc is rather different from that of Glc, AltNAc residue of the PA-0 derivative may affect the interaction between the neighboring Glc residue and the corresponding subsite. To clarify the importance of each subsite more in detail, we are planning to investigate further by using other PA-0 derivatives

having one slightly modified Glc residue (e.g., 2-deoxy-Glc, 3-deoxy-Glc, or 6-deoxy-Glc).

The abovementioned substrate specificity of GP results in the formation of the maltotetraosyl- (Glc_4 -) branch. This product specificity of GP should be considered with the substrate specificity of the downstream enzyme GDE [6, 9, 10, 41, 42]. GDE has two distinct catalytic sites on a single polypeptide chain, corresponding to 4- α -glucanotransferase and amylo- α -1,6-glucosidase. It is generally accepted that GDE 4- α -glucanotransferase removes maltotriosyl- (Glc_3 -) residue from the lateral maltotetraosyl- (Glc_4 -) branch via transglycosylation to expose a 6- O - α -glucosyl residue and then amylo- α -1,6-glucosidase hydrolyzes the α -1,6-glycosidic linkage of the product. Previously, we analyzed the donor substrate specificity of porcine liver GDE 4- α -glucanotransferase using a set of

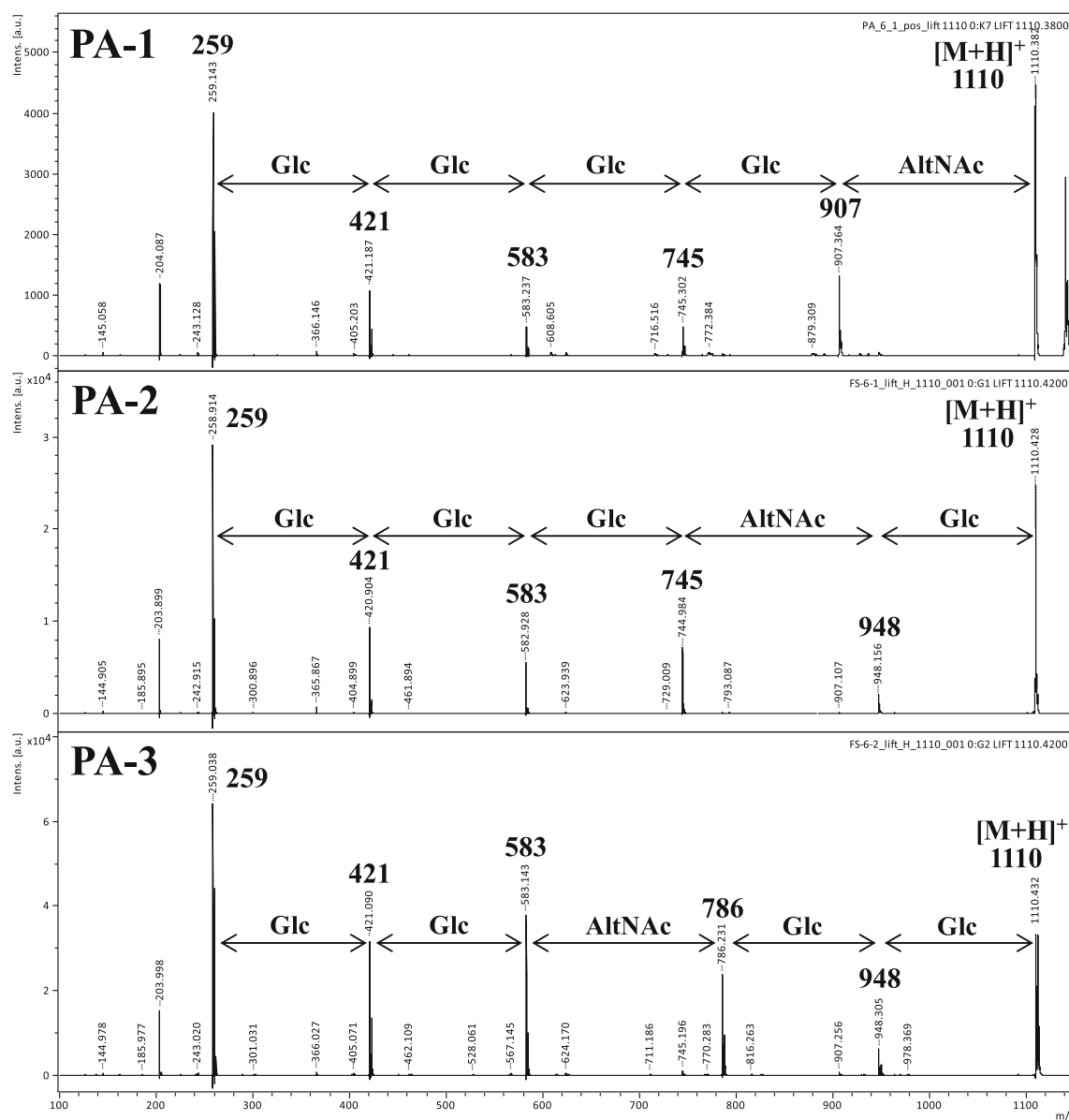


Fig. 4 MS/MS product ion spectra of PA-0 derivatives from the protonated molecules $[M + H]^+$. The chemically synthesized derivatives PA-1, PA-2, PA-3, PA-4, PA-5, and PA-6 have one AltNAc residue at different positions of the oligosaccharide

fluorogenic-branched dextrans with branches of various sizes ($\text{Glc}\alpha 1\text{-4Glc}\alpha 1\text{-4Glc}\alpha 1\text{-4Glc}\alpha 1\text{-4}((\text{Glc}\alpha 1\text{-4})_n\text{-1Glc}\alpha 1\text{-6})\text{Glc}\alpha 1\text{-4Glc}\alpha 1\text{-4Glc}\alpha 1\text{-4GlcPA}$, where $n = 2, 3, 4$ and 5) [43]. The GDE 4- α -glucanotransferase exhibited its maximum activity toward the lateral maltotetraosyl- (Glc_4 -) branch and approximately half maximal activity toward the lateral maltotriosyl- (Glc_3 -) branch; however, little activity was observed toward other branches, particularly toward the lateral maltosyl- (Glc_2 -) branch. Thus, in this study, the product specificity of GP was exactly the same as the donor substrate specificity of the GDE 4- α -glucanotransferase. We think that the SG_{-3} and SG_{-4} subsites in the GP catalytic site prevent the formation of the lateral maltosyl- (Glc_2 -) branch and contribute to the efficient progression of the subsequent GDE catalysis.

Changes in oligosaccharide recognition found in the allosteric regulation of GP

The maltooligosaccharide-binding region of the GP catalytic site recognizes tandem five sugar residues as shown in Fig. 2. By comparing the initial reaction rate toward the PA-0 derivatives ($V_{\text{derivative}}$) with that toward PA-0 ($V_{\text{PA-0}}$), we found that the value of $V_{\text{derivative}}/V_{\text{PA-0}}$ decreased as the level of allosteric activation of GP increased (Table 3 and Fig. 5). For instance, the $V_{\text{derivative}}/V_{\text{PA-0}}$ values for AMP-activated GPb were 4–69 times smaller than those for nonactivated GPb. A similar tendency was observed in the $V_{\text{Glc3-GlcPA}}/V_{\text{PA-0}}$ and $V_{\text{Glc4-GlcPA}}/V_{\text{PA-0}}$ values (Table 3). These results suggest that oligosaccharide recognition at the GP catalytic site is affected by allosteric

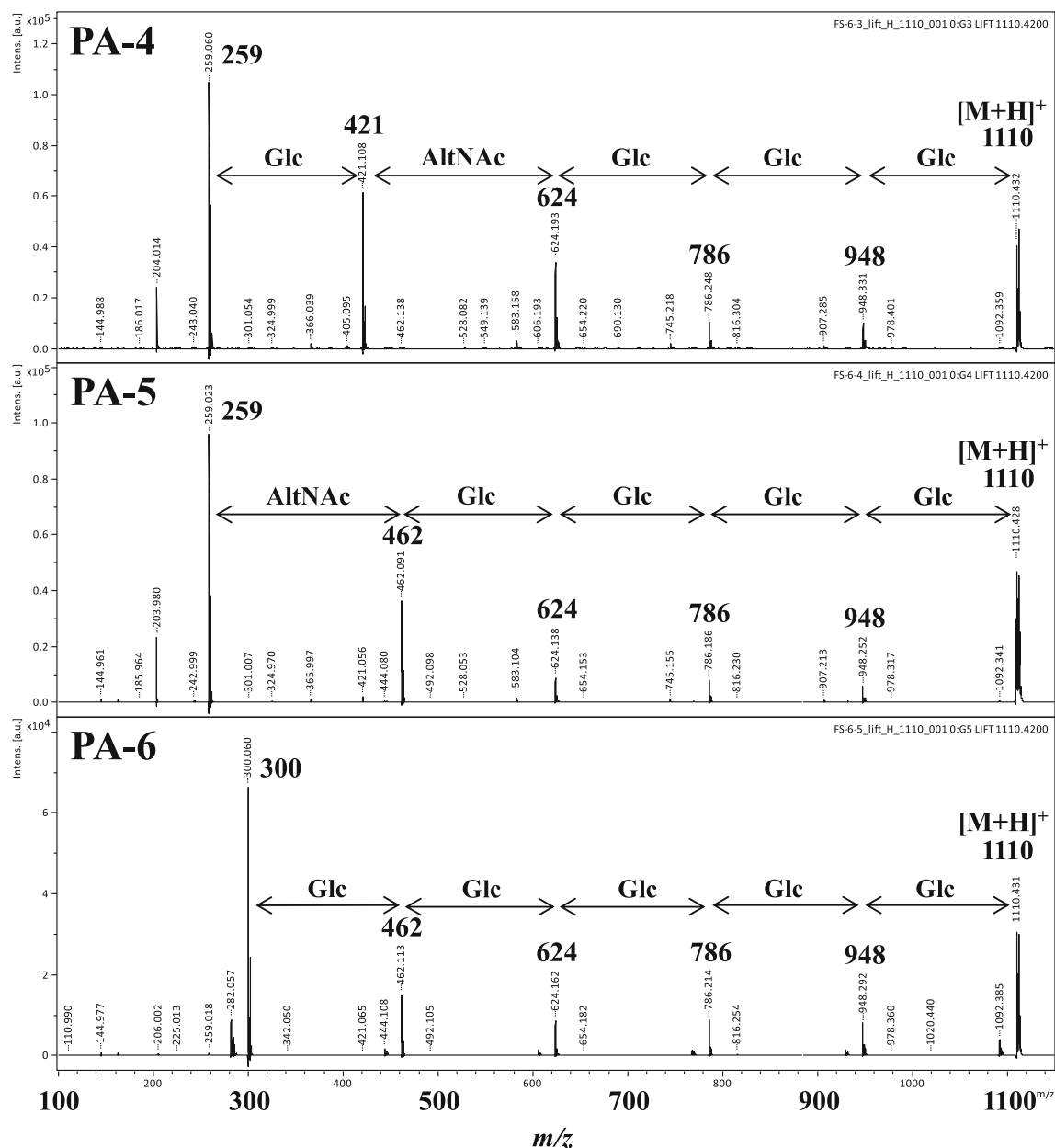


Fig. 4 (continued)

regulation. To investigate this phenomenon from a different point of view, we next analyzed the effect of an allosteric inhibitor on the oligosaccharide recognition by muscle GP α , a partially activated form of the enzyme. For instance, 5-chloroindole-carboxamide derivatives are well known as the allosteric inhibitor of GP; CP-91149 is one of the most active species [44–46]. X-ray crystallographic studies indicate that the indolecarboxamide molecule is accommodated in each of the two new inhibitor sites located inside the central cavity between the two GP subunits [44, 47]. We wanted to know whether the $V_{\text{derivative}}/V_{\text{PA-0}}$ value for the GP α –CP-91149 complex was higher than that for the native GP α . First, we estimated the K_d value of rabbit muscle GP α –CP-91149

binding using the equilibrium dialysis method reported previously (Table 4) [36]. The apparent K_d value estimated was 0.75 μM , which was similar to the IC_{50} value toward human liver GP α (1 μM) [45]. Next, the catalytic site of rabbit muscle GP α was probed with PA-0 and its derivatives in the presence of 50 μM CP-91149, where the enzyme (500 nM or less) was saturated with CP-91149. These results are also summarized in Table 3. The fact that the $V_{\text{derivative}}/V_{\text{PA-0}}$ value for the GP α –CP-91149 complex stood in the middle of the values for GP α and nonactivated GP β (Table 3 and Fig. 5) supported the notion that the $V_{\text{derivative}}/V_{\text{PA-0}}$ value decreased significantly as the level of allosteric activation increased. This systematic change in the recognition of oligosaccharide substrates

Table 3 Phosphorolysis rates of PA-oligosaccharides by rabbit muscle GP

Substrate	Relative initial reaction rate ^a							
	AMP-activated GPb ^b		GPa		Nonactivated GPb		GPa-CP-91149 complex ^c	
Glc ₃ -GlcPA	0.000114	± 0.000009	0.00012	± 0.00002	0.0061	± 0.0004	0.00160	± 0.00008
Glc ₄ -GlcPA	0.0148	± 0.0009	0.0226	± 0.0009	0.058	± 0.003	0.041	± 0.001
Glc ₅ -GlcPA (PA-0)	1.00	± 0.06 ^{d, e}	1.00	± 0.04 ^{d, f}	1.00	± 0.04 ^{d, g}	1.00	± 0.01 ^{d, h, i}
PA-1	0.000015	± 0.000002 ^{j, k}	0.000030	± 0.000002 ^{j, k, l}	0.00104	± 0.00005 ^{j, m}	0.000215	± 0.000004 ^{j, l, m}
PA-2	0.00023	± 0.00001 ⁿ	0.00029	± 0.00001 ^{n, o}	0.0079	± 0.0003 ^p	0.00204	± 0.00003 ^{o, p}
PA-3	0.00086	± 0.00005 ^q	0.00103	± 0.00006 ^{q, r}	0.0130	± 0.0006 ^s	0.0075	± 0.0002 ^{r, s}
PA-4	0.00090	± 0.00006 ^t	0.00143	± 0.00006 ^{t, u, v}	0.014	± 0.002 ^u	0.0128	± 0.0003 ^v
PA-5	0.0066	± 0.0001 ^w	0.0106	± 0.0006 ^{w, x, y}	0.029	± 0.003 ^x	0.023	± 0.001 ^y

^a Values are the rates relative to the rate for PA-0 at 35 μM. Each value shows the mean ± SD (*n* = 3)

^b GPb activity was assayed in the presence of 1 mM AMP

^c GPa activity was assayed in the presence of 50 μM CP-91149

^d No enzymatic activity was observed when P_i was omitted from the assay medium

^e The initial reaction rate was 51.7 nmol Glc₄-GlcPA/(min-mg protein)

^f The initial reaction rate was 19.0 nmol Glc₄-GlcPA/(min-mg protein)

^g The initial reaction rate was 217 pmol Glc₄-GlcPA/(min-mg protein)

^h The initial reaction rate was 1.72 nmol Glc₄-GlcPA/(min-mg protein)

ⁱ No significant difference was observed between 40 and 50 μM CP-91149

^j Glc₃-GlcPA (secondary product) was also observed because Glc₄-GlcPA (primary product) was phosphorolyzed much faster than PA-1

^{k-y} Values followed by the same letter are significantly different (*p* < 0.05)

suggests that some conformational changes have occurred in the maltooligosaccharide-binding region of the GP catalytic site during allosteric regulation.

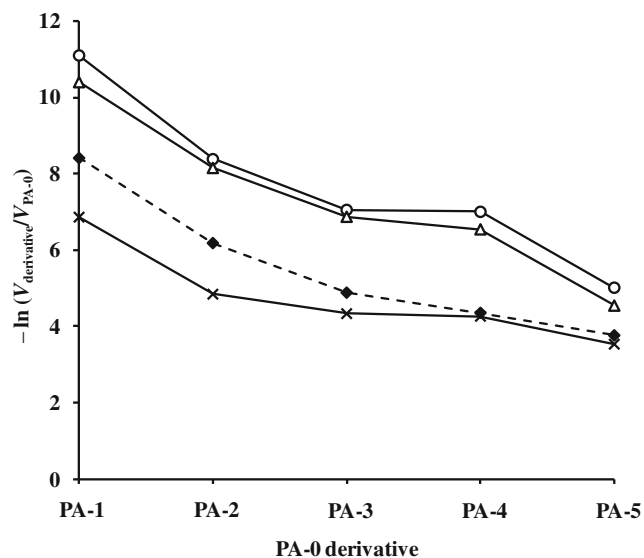


Fig. 5 Effect of the AltNAc residue position on the GP activity. Using GPs at various levels of allosteric modulation, the initial reaction rates toward PA-0 derivatives were compared with those toward PA-0. AMP-activated GPb, open circle; GPa, opened triangle; nonactivated GPb, cross; GPa-CP-91149 complex, filled diamond. A logarithmic scale is used for the ordinate to show a wide range of the $V_{\text{derivative}}/V_{\text{PA-0}}$ values

GP was the first allosteric enzyme to be studied in detail. X-ray crystallographic studies have revealed that the allosteric activation of rabbit muscle GPb is derived from three structural changes: (i) rotation of the *N*- and *C*-terminal domains; (ii) movement of the catalytic site gate; and (iii) a structural change in SP [37, 38]. The structural changes (i) and (ii) were reported to make the catalytic site more accessible to the oligosaccharide and P_i. In the case of the structural change (iii), Arg⁵⁶⁹ was reported to move into a more suitable position for the binding of P_i. In contrast, Barford and Johnson reported from their crystallographic analyses of activated and nonactivated muscle GPBs that no significant structural change existed in the maltooligosaccharide-binding region of the catalytic site by allosteric activation [37]. With regard to Barford and Johnson's data, Buchbinder *et al.* suggested that the activated muscle GPb did not crystallize as the true functional

Table 4 Dissociation constant of GPa-CP-91149 binding

CP-91149 concentration in external solution (μM) ^a	Apparent K_d (μM)
3.0 ± 0.2	0.75 ± 0.49
	- 0.37

^a The equilibrium dialysis experiment was performed as described in *Materials and methods*. Each value shows the mean ± SD (*n* = 3)

dimer [38]. They speculated that additional structural changes are necessary for the allosteric activation of muscle GPb [38]. In this study, using muscle GP with specifically modified maltohexaose derivatives, we found a new possibility that there existed some structural changes in the maltooligosaccharide-binding region of the GP catalytic site during allosteric regulation.

In this study, we prepared a series of specifically modified maltohexaose derivatives with structures that were successfully identified by MALDI MS/MS spectra. Using these compounds as probes, we evaluated the importance of each subsite in the maltooligosaccharide-binding region of the GP catalytic site and proposed a new possibility that the allosteric regulation affected the oligosaccharide recognition at the GP catalytic site. To the best of our knowledge, this is the first report to systematically investigate the oligosaccharide recognition at the GP catalytic site. We think that these series of specifically modified linear maltooligosaccharides can be used as valuable probes to study the catalysis of dextrin-degrading enzymes.

Compliance with ethical standards

Conflict of interest Authors declare no conflicts of interest.

Ethical approval This article does not contain any studies with human participants or animals performed by any of the authors.

References

- Sillerud, L.O., Shulman, R.G.: Structure and metabolism of mammalian liver glycogen monitored by carbon-13 nuclear magnetic resonance. *Biochemistry*. **22**, 1087–1094 (1983)
- Matsui, M., Kakuta, M., Misaki, A.: Comparison of the unit-chain distributions of glycogens from different biological sources, revealed by anion exchange chromatography. *Biosci Biotechnol Biochem*. **57**, 623–627 (1993)
- Roach, P.J., Depaoli-Roach, A.J., Hurley, T.D., Tagliabracci, V.S.: Glycogen and its metabolism: some new developments and old themes. *Biochem J*. **441**, 763–787 (2012)
- Titani, K., Koide, A., Hermann, J., Ericsson, L.H., Kumar, S., Wade, R.D., Walsh, K.A., Neurath, H., Fisher, E.H.: Complete amino acid sequence of rabbit muscle glycogen phosphorylase. *Proc Natl Acad Sci U S A*. **74**, 4762–4766 (1977)
- Tagaya, M., Fukui, T.: Catalytic reaction of glycogen phosphorylase reconstituted with a coenzyme-substrate conjugate. *J Biol Chem*. **259**, 4860–4865 (1984)
- Gordon, R.B., Brown, D.H., Brown, B.I.: Preparation and properties of the glycogen-debranching enzyme from rabbit liver. *Biochim Biophys Acta*. **289**, 97–107 (1972)
- Nakayama, A., Yamamoto, K., Tabata, S.: Identification of the catalytic residues of bifunctional glycogen debranching enzyme. *J Biol Chem*. **276**, 28824–28828 (2001)
- Sato, S., Ohi, T., Nishino, I., Sugie, H.: Confirmation of the efficiency of vitamin B₆ supplementation for McArdle disease by follow-up muscle biopsy. *Muscle Nerve*. **45**, 436–440 (2012)
- Voet, D., Voet, J.D.: *Biochemistry* (third edition) pp. 626–656. John Wiley & sons Inc. Hoboken. (2004)
- Berg, J.M., Tymoczko, J.L., Stryer, L.: *Biochemistry* (sixth edition) pp. 592–616. W. H. Freeman and company. N Y. (2007)
- Miyagawa, D., Makino, Y., Sato, M.: Sensitive, nonradioactive assay of phosphorylase kinase through measurement of enhanced phosphorylase activity towards fluorogenic dextrin. *J Biochem*. **159**, 239–246 (2016)
- Madsen, N.B., Shechosky, S., Fletterick, R.J.: Site-site interactions in glycogen phosphorylase *b* probed by ligands specific for each site. *Biochemistry*. **22**, 4460–4465 (1983)
- Lowry, O.H., Schult, D.W., Passonneau, J.V.: Effects of adenylic acid on the kinetics of muscle phosphorylase *a*. *J Biol Chem*. **239**, 1947–1953 (1964)
- Rush, J.W.E., Spriet, L.L.: Skeletal muscle glycogen phosphorylase *a* kinetics: effects of adenine nucleotides and caffeine. *J Appl Physiol*. **91**, 2071–2078 (2001)
- Tanabe, S., Kobayashi, M., Matsuda, K.: Yeast glycogen phosphorylase: kinetic properties compared with muscle and potato enzymes. *Agric Biol Chem*. **52**, 757–764 (1988)
- Kasvinsky, P.J., Madsen, N.B., Fletterick, R.J., Sygusch, J.: X-ray crystallographic and kinetic studies of oligosaccharide binding to phosphorylase. *J Biol Chem*. **253**, 1290–1296 (1978)
- Sprang, S.R., Goldsmith, E.J., Fletterick, R.J., Withers, S.G., Madsen, N.B.: Catalytic site of glycogen phosphorylase: structure of the T state and specificity for α -D-glucose. *Biochemistry*. **21**, 5364–5371 (1982)
- Withers, S.G., Madsen, N.B., Sprang, S.R., Fletterick, R.J.: Catalytic site of glycogen phosphorylase: structural changes during activation and mechanistic implications. *Biochemistry*. **21**, 5372–5382 (1982)
- Hiromi, K.: Interpretation of dependency of rate parameters on the degree of polymerization of substrate in enzyme-catalyzed reactions. Evaluation of subsite affinities of exo-enzyme. *Biochem Biophys Res Commun*. **40**, 1–6 (1970)
- Hiromi, K., Nitta, Y., Numata, C., Ono, S.: Subsite affinities of glucoamylase: examination of the validity of the subsite theory. *Biochim Biophys Acta*. **302**, 362–375 (1973)
- Nitta, Y., Mizushima, M., Hiromi, K., Ono, S.: Influence of molecular structures of substrates and analogues on taka-amylase catalyzed hydrolyses. I Effect of chain length of linear substrates *J Biochem*. **69**, 567–576 (1971)
- Konishi, Y., Kitazato, S., Nakatani, N.: Partial purification and characterization of acid and neutral α -glucosidases from preclimacteric banana pulp tissues. *Biosci Biotechnol Biochem*. **56**, 2046–2051 (1992)
- Fujita, K., Tahara, T., Koga, T., Imoto, T.: Enzymatic synthesis of specifically modified linear oligosaccharides from γ -cyclodextrin derivatives. Study on importance of active sites of Taka amylase A. *Bull Chem Soc Jpn*. **62**, 3150–3154 (1989)
- Croft, A.P., Bartsch, R.A.: Synthesis of chemically modified cyclodextrins. *Tetrahedron*. **39**, 1417–1474 (1983)
- Walker, G.J., Whelan, W.J.: The mechanism of carbohydrase action: 8, structures of the muscle-phosphorylase limit dextrans of glycogen and amylopectin. *Biochem J*. **76**, 264–268 (1960)
- Hase, S., Ikenaka, T., Matsushima, Y.: Structure analyses of oligosaccharides by tagging of the reducing end sugars with a fluorescent compound. *Biochem Biophys Res Commun*. **85**, 257–263 (1978)
- Kuraya, N., Hase, S.: Release of O-linked sugar chains from glycoproteins with anhydrous hydrazine and pyridylation of the sugar chains with improved reaction conditions. *J Biochem*. **112**, 122–126 (1992)
- Makino, Y., Omichi, K.: Acceptor specificity of 4- α -glucanotransferases of mammalian glycogen debranching enzymes. *J Biochem*. **139**, 535–541 (2006)
- Natsuka, S., Masuda, M., Sumiyoshi, W., Nakakita, S.: Improved method for drawing of a glycan map, and the first page of glycan

- atlas, which is a compilation of glycan maps for a whole organism. *PLoS One*. **9**, e102219 (2014)
30. Makino, Y., Omichi, K., Hase, S.: Analysis of oligosaccharide structures from the reducing end terminal by combining partial acid hydrolysis and a two-dimensional sugar map. *Anal Biochem*. **264**, 172–179 (1998)
 31. Day, A.G., Parsonage, D., Ebel, S., Brown, T., Fersht, A.R.: Barnase has subsites that give rise to large rate enhancements. *Biochemistry*. **31**, 6390–6395 (1992)
 32. Buckle, A.M., Fersht, A.R.: Subsite binding in an RNase: structure of a barnase–tetranucleotide complex at 1.76-Å resolution. *Biochemistry*. **33**, 1644–1653 (1994)
 33. Burkhardt, G., Wegener, G.: Glycogen phosphorylase from flight muscle of the hawk moth *Manduca sexta*: purification and properties of three interconvertible forms and the effect of flight on their interconversion. *J Comp Physiol B*. **164**, 261–271 (1994)
 34. Makino, Y., Omichi, K.: Sensitive assay of glycogen phosphorylase activity by analysing the chain-lengthening action on a fluorogenic maltooligosaccharide derivative. *J Biochem*. **146**, 71–76 (2009)
 35. Lineweaver, H., Burk, D.: The determination of enzyme dissociation constants. *J Am Chem Soc*. **56**, 658–666 (1934)
 36. Makino, Y., Fujii, Y., Taniguchi, M.: Properties and functions of the storage sites of glycogen phosphorylase. *J Biochem*. **157**, 451–458 (2015)
 37. Barford, D., Johnson, L.N.: The allosteric transition of glycogen phosphorylase. *Nature*. **340**, 609–616 (1989)
 38. Buchbinder, J.L., Rath, V.L., Fletterick, R.J.: Structural relationships among regulated and unregulated phosphorylases. *Annu Rev Biophys Biomol Struct*. **30**, 191–209 (2001)
 39. Leonidas, D.D., Oikonomakos, N.G., Papageorgiou, A.C., Xenakis, A., Cazanias, C.T., Bem, F.: The ammonium sulfate activation of phosphorylase *b*. *FEBS Lett*. **261**, 23–27 (1990)
 40. Ishimizu, T., Hase, S.: Substrate recognition by sugar chain-related enzymes: recognition of a large area of substrates and its strictness and tolerance. *Trends Glycosci Glycotechnol*. **17**, 215–227 (2005)
 41. Okubo, M., Horinishi, A., Takeuchi, M., Suzuki, Y., Sakura, N., Hasegawa, Y., Igarashi, T., Goto, K., Tahara, H., Uchimoto, S., Omichi, K., Kanno, H., Hayasaka, K., Murase, T.: Heterogeneous mutations in the glycogen-debranching enzyme gene are responsible for glycogen storage disease type IIIa in Japan. *Hum Genet*. **106**, 108–115 (2000)
 42. Zhai, L., Feng, L., Xia, L., Yin, H., Xiang, S.: Crystal structure of glycogen debranching enzyme and insights into its catalysis and disease-causing mutations. *Nat Commun*. **7**, 11229 (2016)
 43. Watanabe, Y., Makino, Y., Omichi, K.: Donor substrate specificity of 4- α -glucanotransferase of porcine liver glycogen debranching enzyme and complementary action to glycogen phosphorylase on debranching. *J Biochem*. **143**, 435–440 (2008)
 44. Somsak, L., Czifrak, K., Toth, M., Bokor, E., Chrysina, E.D., Alexacou, K.M., Hayes, J.M., Tiraidis, C., Lazoura, E., Leonidas, D.D., Zographos, S.E., Oikonomakos, N.: New inhibitors of glycogen phosphorylase as potential antidiabetic agents. *Curr Med Chem*. **15**, 2933–2983 (2008)
 45. Martin, W.H., Hoover, D.J., Armento, S.J., Stock, I.A., McPherson, R.K., Danley, D.E., Stevenson, R.W., Barrett, E.J., Treadway, J.L.: Discovery of a human liver glycogen phosphorylase inhibitor that lowers blood glucose *in vivo*. *Proc Natl Acad Sci U S A*. **95**, 1776–1781 (1998)
 46. Lerin, C., Montell, E., Nolasco, T., Garcia-Rocha, M., Guinovart, J.J., Gomez-Foix, A.M.: Regulation of glycogen metabolism in cultured human muscles by the glycogen phosphorylase inhibitor CP-91149. *Biochem J*. **378**, 1073–1077 (2004)
 47. Oikonomakos, N.G., Chrysina, E.D., Kosmopoulou, M.N., Leonidas, D.D.: Crystal structure of rabbit muscle glycogen phosphorylase *a* in a complex with a potential hypoglycaemic drug at 2.0 Å resolution. *Biochim Biophys Acta*. **1647**, 325–332 (2003)